

Cooling rate dependence of the antiferromagnetic domain structure of a single crystalline charge ordered manganite.

R. Mathieu and P. Nordblad

Department of Materials Science, Uppsala University, Box 534, SE-751 21 Uppsala, Sweden

A. R. Raju and C. N. R. Rao

Chemistry and Physics of Materials Unit, Jawaharlal Nehru Centre for Advanced Scientific Research, Jakkur P.O., Bangalore - 560 064, India
(December 2, 2024)

The low temperature phase of single crystals of $\text{Nd}_{0.5}\text{Ca}_{0.5}\text{MnO}_3$ and $\text{Gd}_{0.5}\text{Ca}_{0.5}\text{MnO}_3$ manganites is investigated by squid magnetometry. $\text{Nd}_{0.5}\text{Ca}_{0.5}\text{MnO}_3$ undergoes a charge-ordering transition at $T_{CO}=245\text{K}$, and a long range CE-type antiferromagnetic state is established at $T_N=145\text{K}$. The dc-magnetization shows a cooling rate dependence below T_N , associated with additional magnetic correlations of short range in the low temperature antiferromagnetic state. These correlations yield a weak spontaneous magnetic moment, related to the CE-type antiferromagnetic structure, and to the presence in this state of fully orbital ordered regions separated by orbital domain walls. The observed cooling rate dependence is interpreted to be a consequence of the rearrangement of the orbital domain state induced by the large structural changes occurring upon cooling.

I. INTRODUCTION

Hole-doped manganites $\text{R}_{1-x}\text{A}_x\text{MnO}_3$ ($\text{R}=\text{La},\text{Nd},\text{Pr},\dots$ and $\text{A}=\text{Sr},\text{Ca},\dots$), exhibit colossal magnetoresistive [1,2] (CMR) properties, associated with the mixed manganese valence $\text{Mn}^{3+}(t_{2g}^3e_g^1)/\text{Mn}^{4+}(t_{2g}^3)$ resulting from the substitution of trivalent R ions by x divalent A ions. The $x \sim 0.5$ doping is particularly interesting, since the magnetic interaction is affected by i) the ordering of the Mn^{3+} and Mn^{4+} charges [2,3], commonly referred as charge-ordering (CO), ii) the ordering of the e_g electron orbitals on the Mn^{3+} sites and iii) the coupling between orbital degree of freedom and the lattice. For example, $\text{Nd}_{0.5}\text{Ca}_{0.5}\text{MnO}_3$ (NCMO) undergoes a CO transition [4] at $T_{CO}=245\text{K}$ with partial orbital ordering (OO) and magnetic correlations of short range. At lower temperatures, the OO increases and a long range CE-type [5] antiferromagnetic (AFM) state is established at $T_N=145\text{K}$. An insulator-to-metal transition occurs around this temperature in intermediate ($\sim 5\text{T}$ or higher) magnetic fields [4]. The CE-type phase involves both FM and AFM interactions. It consists of ferromagnetic (FM) chains in the (a,b) plane, AFM coupled between each other within this plane, and along the c -axis. Neutrons [6] and Brillouin [7] scattering experiments detect additional FM correlations in the low temperature CE-type AFM phase. Also resistivity noise measurements reveal two-level fluctuations [8] related to the phase separation scenario [9], including mixed-phase states of different magnetic and electrical properties. In this context, the observed magnetic field induced metal-insulator transition [10] reflects the percolative growth of conducting FM clusters embedded in an AFM matrix [11].

In the present article, we investigate the stability of the low temperature AFM phase of a $\text{Nd}_{0.5}\text{Ca}_{0.5}\text{MnO}_3$ single crystal using ac and dc magnetization measurements. The zero field cooled (ZFC) and field cooled (FC) mag-

netization are recorded vs. temperature and time after specific cooling protocols. Similar measurements are performed on a $\text{Gd}_{0.5}\text{Ca}_{0.5}\text{MnO}_3$ (GCMO) single crystal for comparison. GCMO also shows charge-ordering at $T_{CO}=260\text{K}$, but no long range AFM, and remains insulating at all temperatures, even in large magnetic fields [12]. In the case of NCMO, the magnetization appears cooling rate dependent below T_N , revealing additional magnetic correlations in the AFM state associated with a weak spontaneous moment. The corresponding excess magnetization seems connected to the CE-type structure, and to the large structural changes occurring upon cooling. The results indicate that the excess magnetization that appears along the zig-zag chains of the CE-Type structure is of short range, and related to the presence of domain walls in the (a,b) plane breaking the orbital coherency.

II. SAMPLES AND EXPERIMENTS

Single crystals of NCMO [7] and GCMO were grown using floating zone furnace (NEC, Japan). Temperature and time dependent zero field cooled (ZFC) and field cooled (FC) magnetizations measurements were performed using a Quantum Design MPMS5 Superconducting QUantum Interference Device (SQUID) magnetometer. In the ZFC and FC case, the magnetization M was collected on re-heating in a small magnetic field $H=20\text{ Oe}$ after slow (3K/min) and fast (60K/min) cooling from room temperature down to 5K. Additional ac-susceptibility χ measurements ($f=125\text{Hz}$, $h=20\text{ Oe}$) were recorded using the same cooling protocol on a Lakeshore 7225 susceptometer for comparison. The volume susceptibility - ' M/H ' (dc) or χ (ac) - is plotted in the following in dimensionless (SI) units.

III. RESULTS AND DISCUSSION

Figure 1 shows the cooling rate dependence of the ZFC and FC magnetization for NCMO. (a) shows the temperature dependence of the ZFC (markers) and FC (simple line) magnetization, measured on re-heating after fast (continuous lines) and slow (dotted) cooling. In the case of fast cooling or quench to low temperatures, an excess magnetization ΔM appears below T_N , both in the ZFC and FC curves, reflecting the presence of additional magnetic correlations within the long range AFM state. The difference plots of the FC and ZFC curves (same symbols as in the main frame) are added in the insert, showing that the excess magnetization ΔM [$=M(\text{fast cooling}) - M(\text{slow cooling})$] appears slightly below T_N , around $T=130\text{K}$. In our weak probing field, ΔM amounts to $2.88 \times 10^{-5} \mu_B/\text{f.u}$ at $T=35\text{K}$. M vs. H measurements up to higher fields (4000 kA/m) recorded after fast (continuous line) and slow (dotted line) cooling to $T=35\text{K}$ are shown in Figure 2. In both cases, a closely linear field dependence of the magnetization is observed, reflecting the long range AFM ordering. The comparison of the two curves (see insert) yields a weak spontaneous moment of $4.46 \times 10^{-4} \mu_B/\text{f.u}$.

The excess magnetization relaxes with time, as illustrated in Figure 1(b): As in Fig. 1(a), the ZFC magnetization is recorded on reheating from the lowest temperature (pointer **1** on the figure) up to **2** (circles), below T_N . The sample is cooled back (3K/min) to **1** and M recorded on re-heating up to **3** (crosses), corresponding to temperatures above T_N . The sample is again cooled down (3K/min) to **1**, and M is once again recorded up to **3** (simple line). The ZFC curves obtained in (a) are added as dotted lines for comparison. As expected, both the first (from **1** to **2** after a fast cooling) and the last (from **1** to **3** after a slow cooling) measurements coincide with the earlier results shown in (a). The second measurement, recorded from **1** to **3** after a stop **2**, yields instead a lower ΔM , showing that the excess magnetization is relaxing with time. It should be stressed that only a small dc-magnetic field, acting as a non perturbing probe of the system, is used to record the magnetization; i.e. the observed effects are not driven by the magnetic field employed in the experiments [13]. To evidence this, we show in insert of Fig. 1(b) the temperature dependence of the in-phase component of the ac-susceptibility recorded under the same conditions as the ZFC and FC magnetizations, after fast (simple line) and slow (dotted line) cooling; a similar cooling rate dependence is observed in the ac-susceptibility. In the above described measurements, M was recorded using a magnetic field directed along the c -axis of NCMO. Figure 2(a) shows the corresponding results on the ZFC magnetization measured in the (a,b) plane. The cooling rate dependence is again observed, but the excess magnetization has a smaller magnitude, as seen in the main frame but also in the insert where the difference plots of the ZFC curves

for the two different orientations of H are shown. This could indicate that most of the excess magnetization lies along the c direction. Since the single crystals show no sign of twinning, the lower magnitude of ΔM could also be attributed to some magnetic anisotropy in the (a,b) plane.

In the case of GCMO, the cooling rate dependence is not observed, and the magnetizations curves recorded along c after slow and fast cooling virtually coincide, as shown in Fig. 2(b). On the other hand, the ZFC and FC curves deviate from each other below $T \sim 100\text{K}$, indicating irreversibility below this temperature, and thus the development of magnetic correlation. The insert of Fig. 2(b) shows the normalized difference between the ZFC and FC curves for both GCMO and NCMO, which is a measure of the irreversibility. In the case of NCMO, the irreversibility arises sharply at T_N , while it appears more gradually in GCMO. The magnetic correlation developing below $T \sim 100\text{K}$ seems to remain of short range, as in the very similar $\text{Y}_{0.5}\text{Ca}_{0.5}\text{MnO}_3$ [14] manganite. The cooling rate dependence of the magnetization in NCMO is thus related to the long range AFM state established at low temperatures. The excess moment is connected to the CE-Type structure, possibly via the large increase in orthorhombic distortion [12] and c -axis contraction [4] occurring between T_{CO} and T_N upon cooling. Local defects in the perfect antiferromagnetic arrangement then yield the observed spontaneous moment.

To further elucidate the dynamic nature of the magnetization of NCMO, we have performed FC-relaxation experiments, employing different thermal protocols: (0). the sample is first rapidly cooled (fast cooling rate) to the measurement temperature $T_m=35\text{K} < T_N$ in $H=20$ Oe, and after a short waiting time of $\sim 20\text{s}$ (necessary to achieve temperature stability), the magnetization is recorded vs. time. (1). The sample is first rapidly cooled to the lowest temperature, and the FC-relaxation collected after re-heating to T_m . The temperature dependence of the magnetization is recorded during the re-heating to T_m and above. (2). The sample is rapidly cooled to T_m , from where the cooling proceeds with a slower rate, and the magnetization is always recorded vs. temperature. The FC relaxation is collected after re-heating to T_m . As in 1, the magnetization is recorded during the re-heating. (3) is similar to 2, but using a slower cooling rate. In all case, M is recorded during $t_m=10000\text{s}$ at T_m . The results are plotted vs. temperature in Fig. 3(a), and the corresponding relaxation curves are shown in Fig. 3(b). 0 and 1 are nearly identical, showing again that the cooling rate through T_N is the key parameter of our effect. As observed earlier in Fig. 1(b), the relaxation diminishes when the effective cooling slows down, from 0/1 to 3. This relaxation reflects the growth in size or length of the magnetic correlations observed in the AFM state.

Neutron powder diffraction studies on a similar charge and orbital ordered CE-Type AFM manganite [15] indicate magnetic disorder in the Mn^{3+} sublattice, associ-

ated to domain boundaries breaking the long range orbital ordering. Recent x-ray scattering results [16] also indicate a partial orbital ordering of the low temperature phase, leading to an orbital domain state. The orbital ordered parts of the zig-zag chains of the CE-Type structure would appear as small FM clusters [17,3]. The cooling rate dependence here observed below T_N could thus be related to the intrinsic inhomogeneities of the CE-Type structure, and the rearrangement of orbital domains and domain walls to accommodate the large contraction of the structure occurring upon cooling. The cooling rate determines the time allowed to the system to accomodate the structural modifications governed by the temperature. In a similar way, one can also perturb the CE-type state by introducing impurities in the structure, for example by replacing some of the Mn cations by Cr or Ru [18]. The orbital ordering is again affected, and FM-like correlations induced.

The cooling rate dependence of the FC magnetization depicted in Fig. 3(a) is unusual and deserves some additional comments. In experiment **1**, the magnetization curve always lies above the FC curve obtained for the slow cooling case, closely following the curve obtained for a fast cooling. In experiments **0** and **2** instead, M/H at $T_m=35$ K amounts to 0.0185 [SI] immediatly after a rapid cooling from room temperature and the magnetization curve thus surprisingly remains below the FC curve obtained for a slow cooling. During a fast cooling to T_m , the system can not accomodate the excess moments appearing with the domain walls, and its magnetization remains lower than in the slow cooling case. In experiment **1**, the sample is re-heated T_m , after a rapid cooling down, allowing the excess moment to further develop, yielding the high magnetization value. The relaxation curves corresponding to experiments **0** and **1** shown in Fig.3 (b) appear almost identical, which indicates that a similar magnetic configuration is probed in both experiments, albeit with a different initial magnetization level.

IV. CONCLUSION

The magnetization of a single crystal of the charge ordered manganite $\text{Nd}_{0.5}\text{Ca}_{0.5}\text{MnO}_3$ is cooling rate dependent below T_N . The results indicate the presence of additional magnetic correlations of short range associated with a weak spontaneous moment, related to the CE-type magnetic structure and its inhomogeneities. Such correlations could be associated with “ferromagnetic clusters”, and correspond to fully orbital ordered parts of the CE-type zig-zag chains, separated by orbital domain walls. The cooling rate is then used to probe the orbital state, and study how it accommodates the large structural transformation occurring upon cooling.

The application of a large magnetic field would increase the size of the FM-like correlations and yield the observed insulator-metal transition below T_N . For comparison, in

the case of $\text{Gd}_{0.5}\text{Ca}_{0.5}\text{MnO}_3$, no long range antiferromagnetism is established at any temperature, and neither a cooling rate dependence nor an insulator-metal transition is observed.

ACKNOWLEDGMENTS

Financial support from the Swedish Natural Science Research Council (NFR) is acknowledged.

- [1] A. P. Ramirez, *J. Phys.: Condens. Matter* **9**, 8171 (1997).
- [2] C. N. R. Rao, A. Arulraj, A. K. Cheetham and B. Raveau, *J. Phys.: Condens. Matter* **12** R83-R106 (2000).
- [3] S. Krupička, M. Maryško, Z. Jirák, J. Hejtmánek, *J. Magn. Magn. Mater.* **206**, 45-67 (1999).
- [4] T. Vogt, A. K. Cheetham, R. Mahendiran, A. K. Raychaudhuri, R. Mahesh and C. N. R. Rao, *Phys. Rev. B* **54**, 15303 (1996)
- [5] J. B. Goodenough, *Phys. Rev.* **100**, 564 (1955).
- [6] P. G. Radaelli, D. E. Cox, M. Marezio, S.-W. Cheong, P. E. Schiffer, and A. P. Ramirez, *Phys. Rev. Lett.* **75**, 4488 (1995).
- [7] P. Murugavel, C. Narayana, A. K. Sood, S. Parashar, A. R. Raju, and C. N. R. Rao, *Europhys. Lett.* **52**, 461 (2000).
- [8] B. Raquet, A. Anane, S. Wirth, P. Xiong, and S. von Molnár, *Phys. Rev. Lett.* **84**, 4485 (2000).
- [9] A. Moreo, S. Yunoki, and E. Dagotto, *Science* **283**, 2034 (1999); E. Dagotto, T. Hotta, and A. Moreo, *cond-mat/0012117*.
- [10] M. Tokunaga, N. Miura, Y. Tomioka, and Y. Tokura, *Phys. Rev. B* **57**, 5259 (1998).
- [11] V. Podzorov, M. Uehara, M. E. Gershenson, T. Y. Koo, and S.-W. Cheong, *Phys. Rev. B* **61**, R3784 (2000).
- [12] A. Arulraj, P. N. Santhosh, R. Srinivasa Gopalan, A. Guha, A. K. Raychaudhuri, and C. N. R. Rao, *J. Phys.: Condens. Matter.* **10**, 8497 (1998).
- [13] The CO-AFM state of NCMO has also been investigated by studying the relaxation of the magnetization and electrical resistance after large magnetic field changes by T. Kimura et al., *Phys. Rev. Lett.* **83**, 3940 (1999). We here study intrinsic properties of the magnetic configuration of NCMO and GCMO, monitoring the relaxation of the magnetization employing a small non-perturbing magnetic field.
- [14] A. Arulraj, R. Gundakaram, A. Biswas, N. Gayathri, A. K. Raychaudhuri, and C. N. R. Rao, *J. Phys.: Condens. Matter.* **10**, 4447 (1998).
- [15] P. G. Radaelli, D. E. Cox, M. Marezio, S.-W. Cheong, *Phys. Rev. B* **55**, 3015 (1997).
- [16] J. P. Hill et al. *Cond-mat/0105064*
- [17] K. H. Kim, M. Uehara, and S.-W. Cheong, *Phys. Rev. B* **62**, R11945 (2000).

[18] C. Martin et al., Phys. Rev. B **63**, 174402 (2001); M. Hervieu et al., *cond-mat/0010427*.

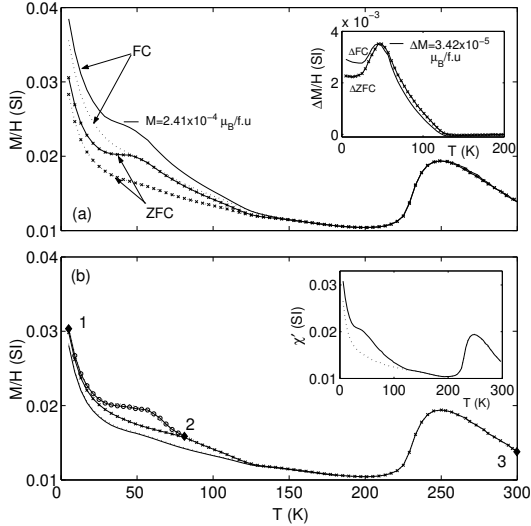


FIG. 1. Temperature dependence of the ZFC (markers) and FC (simple line) magnetizations of NCMO; $H=20$ Oe. (a) The magnetization is recorded on re-heating along the c-axis after fast (continuous line) and slow (dotted line) coolings down to 5K. The corresponding value of $M_{FC}(T=35K)$ in $\mu_B/f.u$ is added for comparison. The insert shows the difference plots of the FC and ZFC magnetization curves (same symbols as in the main frame). (b) Idem adding a cooling and re-heating to temperatures below T_N (see main text). The insert shows the cooling rate dependence of the ac-susceptibility of NCMO, recorded vs. temperature using a small ac-field, after similar fast and slow coolings. $h=20$ Oe, $f=125$ Hz. The simple line corresponds to the fast cooling case, the dotted one to the slower one. The maximum value of ΔM in $\mu_B/f.u$ is added.

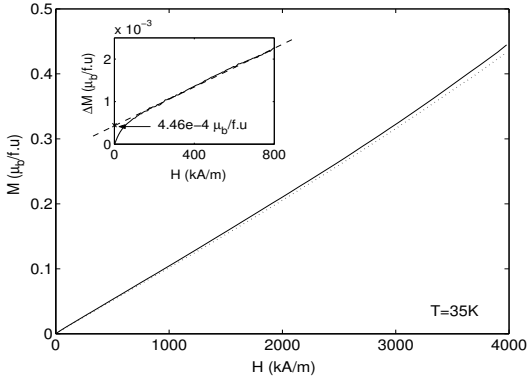


FIG. 2. M vs. H up to high magnetic fields recorded after fast (continuous line) and slow (dotted line) cooling of NCMO; $T=35$ K. The insert shows the corresponding ΔM [$=M(\text{fast cooling}) - M(\text{slow cooling})$] difference plot.

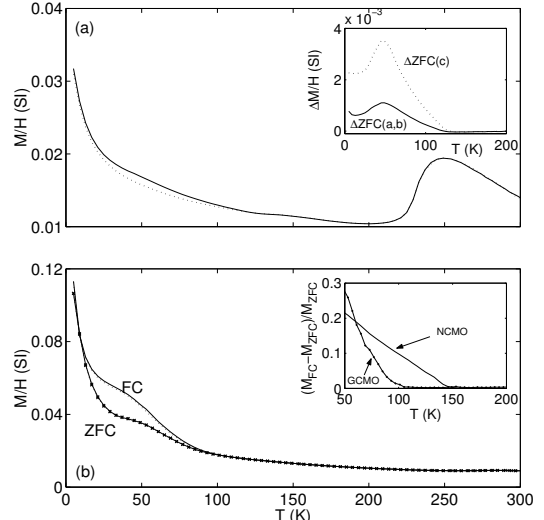


FIG. 3. (a) Temperature dependence of the ZFC magnetization for NCMO. The magnetization in the (a,b)-plane is recorded on re-heating after fast (continuous line) and slow (dotted line) cooling to 5K. The insert shows the corresponding difference plot. The curve obtained when measuring along the c direction (c.f. insert of Fig. 1(a)) is added. (b) Corresponding results for GCMO. M is measured along the c-axis and both ZFC (markers) and FC (simple line) are measured with fast (continuous line) and slower (dotted line) cooling rates. The insert shows the temperature dependence of the irreversibility observed in the magnetization curves of NCMO and GCMO.

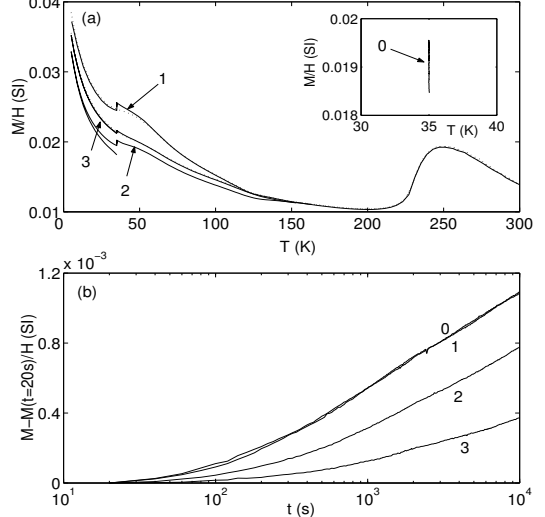


FIG. 4. Temperature dependence of the FC magnetization for NCMO. Intermediate temperature stops are made during the cooling and heating at $T_m=35$ K (see text) (a) shows the results plotted vs. temperature, as well as the 'reference' FC curves from Fig. 1(a) in dotted lines. "0" is plotted separately for clarity; M was only recorded vs. time in this experiment. (b) shows the the relaxation of magnetization during t_m at $T_m=35$ K.